Rare Metal Materials and Engineering
Volume 51, Issue 5, May 2022
Available online at www.rmme.ac.cn

Science Press

Cite this article as: San Zhanyi, Liu Shengfa, Liu Zhibo, et al. Microstructural Characteristics and Mechanical Behavior of Work-Hardened Al-10wt% Mg Alloy Subjected to Low Temperature Annealing[J]. Rare Metal Materials and Engineering, 2022, 51(05): 1550-1557.

ARTICLE

Microstructural Characteristics and Mechanical Behavior of Work-Hardened Al-10wt% Mg Alloy Subjected to Low Temperature Annealing

San Zhanyi[1], Liu Shengfa[1], Liu Zhibo[1], Lin Yaojun[1], Liu Manping[2]

[1] School of Materials Science and Engineering, Wuhan University of Technology, Wuhan 430070, China; [2] School of Materials Science and Engineering, Jiangsu University, Zhenjiang 212013, China

Abstract: The Al-10wt% Mg alloy was cold-rolled with the thickness reduction ratio of 75% followed by annealing at 75~150 °C, and its microstructure characteristics and mechanical behavior were investigated. The as-rolled and annealed Al-10wt% Mg alloys are characterized by elongated ultra-fine grains, high density of dislocations, a very small amount of Al_3Mg_2 phase, and no dispersed distribution of Al_3Mg_2 phase. With increasing the annealing temperature, the width of elongated ultra-fine grains is increased and the dislocation density is decreased. After annealing at 75~150 °C, compared with those of as-rolled alloys, the yield strength of annealed alloys is decreased by 8%~33%, the ultimate tensile strength is decreased by 1%~12%, and the elongation is increased by 16%~83%. The contributions of various strengthening mechanisms to yield strength and the contributions of preexisting dislocations and Mg solute to ductility were analyzed and discussed.

Key words: Al-Mg alloys; cold rolling; annealing; strength; ductility

The commercial 5000 series wrought Al-Mg alloys with 1wt% ~5wt% Mg have been widely used as structural components in aircrafts and ground transportation vehicles due to their low mass densities, excellent corrosion resistance, and good weldability[1-3]. As the non-heat treatable wrought Al alloys, the strengthening mechanisms in 5000 series Al-Mg alloys primarily involve the solid-solution strengthening, dislocation strengthening (work-hardening), and grain boundary (GB) strengthening. Over the past decade, the wrought Al-Mg alloys with >5wt% Mg attract much attention[4-6], due to their further reduced mass densities and simultaneously increased strength originating from the enhanced solid-solution, GB, and dislocation strengthening as a result of increased Mg solute contents[7,8], which effectively promotes the energy conservation and gas emission reduction[9]. Zha[7] and Chen[10] et al processed Al-Mg alloys with 6wt% ~10wt% Mg via the severe plastic deformation (SPD) approach, namely equal channel angular pressing (ECAP), at room temperature (RT). Zha et al[7] created the bimodal microstructure consisting of elongated and equiaxed ultra-fine grains (UFGs) and coarse grains (CGs) with a high density of dislocations in the three-pass as-ECAPed Al-7wt% Mg alloy, which exhibited the yield strength (YS) of ~446 MPa, ultimate tensile strength (UTS) of ~507 MPa, and elongation of ~11%. Chen et al[10] prepared the four-pass as-ECAPed Al-6wt% Mg alloy consisting of elongated and equiaxed UFGs with a high density of dislocations, and YS, UTS, and elongation of this alloy were ~562 MPa, ~582 MPa, and ~5.5%, respectively.

Because SPD is difficult to apply in industrial production, the introduction of work hardening via conventional plastic deformation approaches attracts much attention. Zha et al[11] prepared the as-rolled Al-9wt% Mg alloy with the thickness reduction ratio of 75% via only one single pass of ECPA at RT, and found that its bimodal microstructure is similar to that in Ref.[7]. Besides, YS, UTS, and elongation of this alloy are ~355 MPa, ~525 MPa, and ~14%, respectively. However, Jang et al[12] found that although the cold-rolled Al-7wt% Mg,

Received date: May 06, 2021
Foundation item: National Natural Science Foundation of China (U1810108, U1710124)
Corresponding author: Lin Yaojun, Ph. D., Professor, School of Materials Science and Engineering, Wuhan University of Technology, Wuhan 430070, P. R. China, E-mail: yjlin@whut.edu.cn

Al-10wt% Mg, and Al-13wt% Mg alloys with the thickness reduction ratio of 73% acquire the high YS of ~441, ~505, and ~653 MPa and UTS of ~476, ~554, and ~699 MPa, respectively, their elongation is only ~4.1%, ~7.1%, and ~4.9%, respectively. The microstructure of these alloys consists of elongated and equiaxed UFGs with a high density of dislocations. The limited ductility of the as-rolled Al alloys can be primarily attributed to the high density of preexisting dislocations, which results in the increased resistance against the dislocation motion[13] and decreased storage ability of dislocations, thereby leading to the decreased work-hardening ability and then the stain localization (necking) and fracture[14,15]. Therefore, the ductility of the as-rolled Al alloys is inferior. In order to improve the alloy ductility, the annealing is usually performed for plastically deformed Al-Mg alloys with high Mg contents. Lee et al[16] prepared the Al-10wt% Mg alloy through rolling at RT with the thickness reduction ratio of 75% followed by annealing at 450 °C for 1 h, and obtained the fully recrystallized coarse-grained microstructure with average grain size of 21 μm. As a result, the elongation of alloy is increased to ~35%, but YS and UTS are significantly decreased to 170 and 385 MPa, respectively. Feng et al[17] prepared the Al-10wt% Mg alloy by cold-rolling with the thickness reduction ratio of ~67% followed by annealing at temperatures of 170~400 °C for 1 h. After annealing at 170~300 and 350~400 °C, the lamellar structure and equiaxed coarse-grained structure can be obtained, respectively. After annealing at 170 °C, the elongation is increased by ~50%, whereas YS and UTS are only decreased by ~19% and ~6%, respectively, compared with those of the as-rolled alloys. After annealing at 200~300 °C, the elongation increases by 25%~58%, while YS and UTS decrease by 33%~40% and 8%~29%, respectively, compared with those of the as-rolled alloys. After annealing at 350~400 °C, the elongation increases by 2~2.7 times, but YS and UTS decrease by ~60% and 30%~32%, respectively, compared with those of as-rolled alloys. The effect of annealing on plastically deformed Al-10wt% Mg alloys at temperatures lower than 150 °C is rarely investigated. Thus, in this research, the microstructure characteristics and tensile properties of Al-10wt% Mg alloy after cold-rolling with the thickness reduction ratio of 75% followed by annealing at temperatures lower than 150 °C were investigated.

1 Experiment

The mixture of commercial Al (purity>99.9wt%) and Mg (purity>99.9wt%) was induction melted at ~700 °C for 30 min and then poured into a non-preheated cylindrical steel mold with an inner diameter of 60 mm to prepare Al-10wt% Mg ingots. The composition of the as-cast alloy was measured by inductively coupled plasma-optical emission spectrum, as shown in Table 1. The as-cast alloy was solid-solution-treated and homogenized at 425 °C for 9 h followed by water quenching to obtain the single-phase solid solution of Al-10wt% Mg alloy with average grain size of ~160 μm[18]. The Al-10wt% Mg plates after solid-solution treatment and homogenization with the thickness of 2.58 mm were cold-rolled at RT to achieve the final thickness of 0.65 mm, i.e., the total thickness reduction ratio is ~75% at the thickness reduction ratio of ~8% per pass. The as-rolled plates with ~100 mm in length and ~40 mm in width were annealed at 75, 100, and 150 °C for 1 h. For comparison, the as-rolled plate was also annealed at 200 °C for 1 h. During annealing, the thermo-couple node was positioned at the place of 1~2 mm away from the annealed plate center, so the measured temperatures could accurately reflect the real temperatures of the annealed plates.

Table 1 Composition of Al-10wt% Mg alloy (wt%)

Mg	Si	Ca	Fe	Cu	Al
9.98	0.31	0.26	0.06	0.01	Bal.

X-ray diffraction (XRD) analysis of as-cast, as-rolled, and annealed Al-10wt% Mg alloys was performed in Bruker D8 Advance diffractometer using Cu-Kα radiation at 400 mA and 40 kV with the scanning rate of 2°/min and the diffraction angle 2θ of 30°~120°. The microstructures of the as-rolled and annealed Al-10wt% Mg alloys in the planes determined by normal direction (ND) and rolling direction (RD) were characterized by Leica DM2500 M optical microscope (OM) under polarized light. The specimens for OM analysis were prepared firstly by electro-polishing with a solution of 90vol% C_2H_5OH and 10vol% $HClO_4$, and then by anodic oxidation with a solution containing 11 g H_3BO_3, 30 mL HF, and 960 mL H_2O. The microstructures of the as-rolled and annealed Al-10wt% Mg alloys in the planes determined by ND and RD were also studied by JEM-1400 Plus transmission electron microscopy (TEM) operated at 120 kV. The specimens for TEM analysis were prepared by mechanical thinning with the thickness of 30~40 μm, and then treated by twin-jet electro-polishing to achieve electron transparency with a solution composed of 70vol% CH_3OH and 30vol% HNO_3 at −30 °C.

For as-rolled and annealed Al-10wt% Mg alloys, the tensile tests were performed with the initial strain rate of 5×10^{-4} s^{-1} at RT using an Instron-5966 Universal Tester (10 kN) equipped with a video extensometer for accurate measurement of strains. The dog-bone-shaped tensile specimens with the gauge length of 10 mm and a cross-section of 2.5 mm×0.65 mm were used. The normal and tensile directions of a tensile specimen corresponded to ND and RD of the raw material, respectively. At least three specimens were tested for each type of as-rolled and annealed alloys for accuracy.

2 Results and Discussion

2.1 Results

Fig. 1a and 1b show XRD patterns of the as-rolled and annealed Al-10wt% Mg alloys at 2θ=30°~120° and 2θ=35°~45°, respectively. No peak corresponding to Al_3Mg_2 phase can be observed in XRD patterns of as-rolled, 75 °C/annealed, 100 °C/annealed, or 150 °C/annealed Al-10wt% Mg alloys. After annealing at 200 °C, the peaks of Al_3Mg_2 phase can be observed, indicating the precipitation of Al_3Mg_2 phase, which

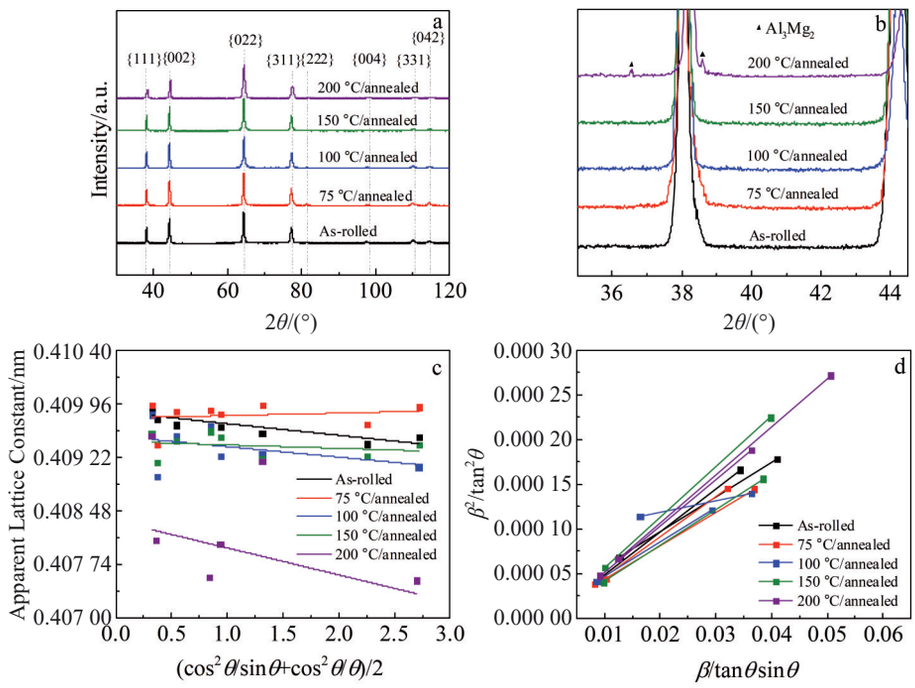

Fig. 1 XRD patterns of as-rolled and annealed Al-10wt% Mg alloys at different temperatures at 2θ=30°~120° (a) and 2θ=35°~45° (b); relationship between apparent lattice constant and $(\cos^2\theta/\sin\theta+\cos^2\theta/\theta)/2$ (c); relationship between $\beta^2/\tan^2\theta$ and $\beta/\tan\theta\sin\theta$ (d)

is consistent with Ref. [17]. Fig. 1c shows the apparent lattice constants $a(\theta)$ of the Al solid-solution matrixes calculated by Bragg equation against the values of Nelson Riley function[19], $(\cos^2\theta/\sin\theta+\cos^2\theta/\theta)/2$, where θ is the Bragg angle. The lattice constant of Al solid-solution matrix is determined by extrapolating the equation $(\cos^2\theta/\sin\theta+\cos^2\theta/\theta)/2=0$, i. e., θ = 90° in the fitting line using the least-square method[19]. The calculated lattice constants are reported in Table 2. Based on the increase by 0.000 46 nm in lattice constant with an increase by 1at% of Mg solute content in Al-Mg alloys[20], the Mg solute content in the as-rolled and annealed Al-10wt% Mg alloys can be estimated using the lattice constant of pure Al with a=0.404 95 nm[20] as the baseline. The estimated Mg solute contents are presented in Table 2. The Mg solute contents in the as-rolled, 75 °C/annealed, 100 °C/annealed, and 150 °C/annealed Al-10wt% Mg alloys are slightly lower than the total Mg content. The other part of Mg may precipitate at GBs or form Al-Mg intermetallics beyond the detection limit of XRD analysis. The Mg solute content of 200 °C/annealed Al-10wt% Mg alloys is 6.68wt% and the other part of Mg forms the Al_3Mg_2 phase.

Based on XRD peak broadening, the microstrain $\langle\varepsilon_x^2\rangle^{1/2}$ and crystalline size L in the as-rolled and annealed Al-10wt% Mg alloys can be evaluated using the equation[21] $\beta^2/\tan^2\theta = (\lambda/L)(\beta/\tan\theta\sin\theta)+16\langle\varepsilon_x^2\rangle$, where β is the integral breadth corresponding to Bragg angle θ after subtraction of instrumental broadening, and the X-ray wavelength is λ = 0.154 06 nm. Herein, $\beta^2/\tan^2\theta$ as a function of $\beta/\tan\theta\sin\theta$ is plotted only for the two diffraction peak pairs {111} - {222} and {200} - {400}, due to the presence of crystallographic texture in both as-rolled and annealed Al-10wt% Mg alloys, and the corresponding $\langle\varepsilon_x^2\rangle^{1/2}$ and L are calculated. Then, the dislocation densities (ρ) are evaluated using the equation[23] $\rho = 2\sqrt{3}\langle\varepsilon_x^2\rangle^{1/2}/bL$, where $b=(\sqrt{2}/2)a$ = 0.286 nm is the value of Burger's vector in the Al alloy. The arithmetic average values of dislocation densities corresponding to {111} - {222} and {200} - {400} diffraction peak pairs are taken as the

Table 2 Lattice constant, Mg solute content, and dislocation density in as-rolled and annealed Al-10wt% Mg alloys at different temperatures

Treatment	Lattice constant/nm	Mg solute content		Dislocation density, ρ/m^{-2}
		at%	wt%	
As-rolled	0.409 84	10.63	9.68	1.85×10^{14}
75 °C/annealed for 1 h	0.409 76	10.46	9.52	1.44×10^{14}
100 °C/annealed for 1 h	0.409 51	9.91	9.02	1.23×10^{14}
150 °C/annealed for 1 h	0.409 44	9.76	8.88	7.04×10^{13}
200 °C/annealed for 1 h	0.408 34	7.36	6.68	4.42×10^{13}

overall dislocation densities, as shown in Table 2.

The engineering stress-strain curves of the as-rolled and annealed Al-10wt% Mg alloys are shown in Fig. 2a, and corresponding tensile properties are summarized in Table 3. The as-rolled Al-10wt% Mg alloy achieves YS, UTS, and elongation of 432 MPa, 515 MPa, and 6.9%, respectively. After annealing at 75 °C, YS and UTS of Al-10wt% Mg alloy decrease by ~8% to 396 MPa and by ~1% to 508 MPa, respectively, and the elongation increases by ~16% to 8.0%, compared with those of the as-rolled alloys. After annealing at 100 °C, the elongation of Al-10wt% Mg alloy increases by ~72% to ~11.9%, whereas YS and UTS decrease by ~23% to 331 MPa and by ~12% to 451 MPa, respectively, compared with those of the as-rolled alloys. After annealing at 150 °C, the elongation of Al-10wt% Mg alloy increases by ~83% to ~12.6%, while YS and UTS decrease by ~33% to 291 MPa and by ~12% to 453 MPa, respectively, compared with those of the as-rolled alloys. After annealing at 200 °C, the elongation of Al-10wt% Mg alloy increases by ~33% to ~9.2%, whereas YS and UTS decrease by ~35% to 282 MPa and by ~10% to 466 MPa, respectively, compared with those of the as-rolled alloys. Thus, the annealing at 200 °C leads to the severest deterioration in strength but not the largest increase in elongation as a result of Al_3Mg_2 precipitation. According to Ref. [24, 25], YS of ⩾300 MPa with elongation of ⩾10% represents the good combination of strength and ductility for wrought Al-Mg alloys. Therefore, in this research, YS of 331 MPa and elongation of 11.9% of 100 °C/annealed Al-10wt% Mg alloys achieve the good combination of strength and ductility. In contrast, the required mechanical properties cannot be attained by annealing at temperatures lower than 75 °C or higher than 150 °C. Interestingly, the serrations can be observed in the stress-strain curves of the as-rolled and annealed Al-10wt% Mg alloys, due to the dynamic strain aging effect which represents the Mg solute-dislocation interactions and thus the impedance of Mg solute against dislocation motion and recovery[26,27]. Fig. 2b shows the work-hardening rate $d\sigma/d\varepsilon$, where σ and ε are true stress and true strain, respectively. The work hardening rate of different alloys are arranged from the smallest to the largest as as-rolled <75 °C/annealed<200 °C/annealed<100 °C/annealed<150 °C/annealed Al-10wt% Mg alloys.

OM microstructures in Fig. 3 display arrays of deformation bands in as-rolled and annealed Al-10wt% Mg alloys. A large number of diffused cell boundaries can be observed, because the Mg solute of high content hinders the dislocation motion and thus the rearrangement of diffused dislocation boundaries into well-defined cell or subgrain boundaries.

Fig. $4a_1$~$4d_1$ show TEM microstructures and selected-area electron diffraction (SAED) patterns of as-rolled, 75 °C/annealed, 100 °C/annealed, and 150 °C/annealed Al-10wt% Mg alloys, respectively. The elongated UFGs with fuzzy GBs can be observed in some local regions, and these elongated UFGs contain a high density of dislocations, especially in dislocation-tangling zones (DTZs), which is in agreement with the results in Table 2. It is noted that the annealing

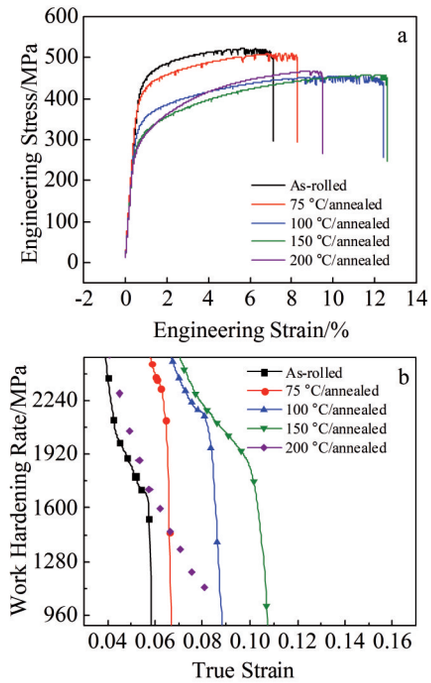

Fig.2 Tensile properties of as-rolled and annealed Al-10wt% Mg alloys at different temperatures: (a) engineering stress-strain curves and (b) work hardening rate-true strain curves

Table 3 Tensile properties of as-rolled and annealed Al-10wt% Mg alloys at different temperatures

Treatment	YS/MPa	UTS/MPa	Elongation/%
As-rolled	432	515	6.9
75 °C/annealed for 1 h	396	508	8.0
100 °C/annealed for 1 h	331	451	11.9
150 °C/annealed for 1 h	291	453	12.6
200 °C/annealed for 1 h	282	466	9.2

temperatures of 75~150 °C are too low for recrystallization occurrence. According to SAED patterns, all ring-like features are attributed to the Al solid-solution matrixes with high angle GBs; a few weak diffraction spots of Al_3Mg_2 phase can be observed, indicating the existence of a very small amount of Al_3Mg_2 phase without dispersion. It is also revealed that the elongated UFGs in annealed alloys have larger width and shorter length than those in the as-rolled alloys do, and the width is increased and the length is slightly decreased with increasing the annealing temperature. This phenomenon can also be confirmed by the distributions of intercept lengths along the direction perpendicular (d_T) and parallel (d_L) to the lamellar boundaries of elongated UFGs. The average intercept lengths along the direction perpendicular to lamellar boundaries ($\bar{d}_T$) of as-rolled, 75 °C/annealed, 100 °C/annealed, and 150 °C/annealed Al-10wt% Mg alloys are 102, 137, 163, and 289 nm, respectively; the average intercept lengths along the direction parallel to lamellar boundaries ($\bar{d}_L$) of as-rolled, 75 °C/annealed, 100 °C/annealed, and 150 °C/annealed

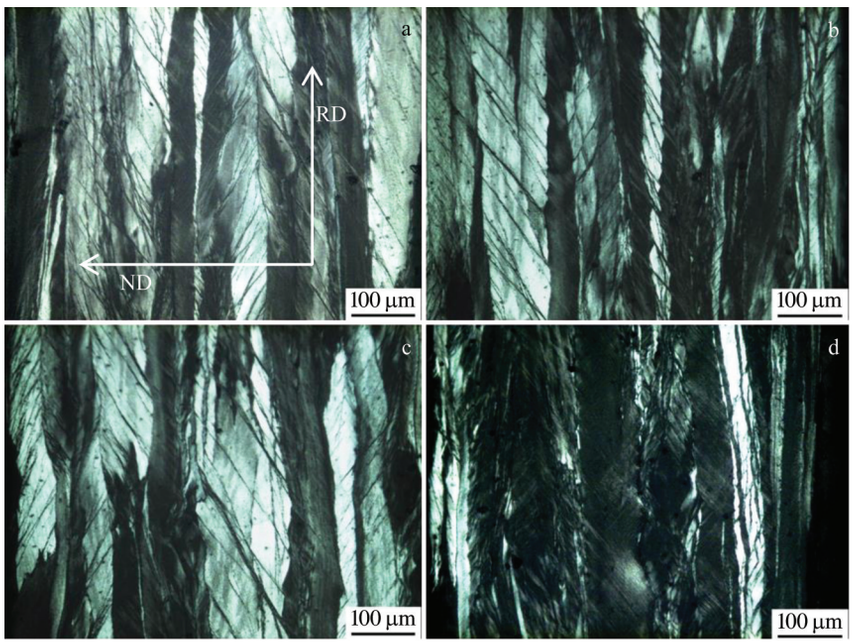

Fig.3 OM microstructures of as-rolled (a), 75 °C/annealed (b), 100 °C/annealed (c), and 150 °C/annealed (d) Al-10wt% Mg alloys

Al-10wt% Mg alloys are 1036, 973, 944, and 926 nm, respectively. The increase in widths of elongated UFGs with increasing the annealing temperature is caused by the migration of lamellar boundaries of elongated UFGs induced by elevated annealing temperatures[28,29]. The decrease in lengths of elongated UFGs may be attributed to the rearrangement of diffused dislocation boundaries into regular subgrain boundaries in some local regions during annealing. It is noted that due to the low annealing temperatures of 75, 100, and 150 °C and strong resistance against dislocation motion caused by Mg solute atoms of 8.88wt% ~9.68wt% , the rearrangement of diffused dislocation boundaries occurs only in very limited local regions where fragmentation of elongated UFGs occurs. Consequently, the length of elongated UFGs only slightly decreases, and elongated UFGs are still featured by diffused boundaries and the absence of well-defined subgrain boundaries.

2.2 Discussion

Due to the small amount of Al_3Mg_2 phase and the absence of dispersed Al_3Mg_2 phase in the as-rolled and annealed Al-10wt% Mg alloys, the strengthening mechanisms primarily involve the solid solution strengthening ($\Delta\sigma_{ss}$), dislocation strengthening ($\Delta\sigma_d$), and GB strengthening ($\Delta\sigma_{gb}$). $\Delta\sigma_{ss}$ can be assessed by $\Delta\sigma_{ss} = HC^n$, where C is the alloy concentration; H and n are material constants of 13.8 MPa/wt% and 1.14 for Al-10wt% Mg alloys[30], respectively. The calculated $\Delta\sigma_{ss}$ is presented in Table 4. $\Delta\sigma_d$ can be evaluated by $\Delta\sigma_d = M\alpha_1 Gb\sqrt{\rho}$, where G=27 GPa is the shear modulus of Al alloys[31], M=3.06 is the Taylor factor[32], and α_1=0.3 is a constant[33]. The calculated $\Delta\sigma_d$ is listed in Table 4. For nanostructured materials, Hall-Petch equation cannot be applied only when the grain size is smaller than a critical value of around 10 nm[34]. In this research, the width and length of elongated UFGs are much larger than the critical value. Therefore, Hall-Petch equation[12] is still applicable, and $\Delta\sigma_{gb}$ can be assessed by $\Delta\sigma_{gb} = K\bar{d}_R$, where K=60 MPa·μm$^{1/2}$ is Hall-Petch slope for Al-Mg alloys[15], and $\bar{d}_R$ is the average boundary spacing of elongated grains. The value of $\bar{d}_R$ can be calculated by $\bar{d}_R = 2/(1/\bar{d}_T + \pi/2\bar{d}_L)$[35]. Then the calculated $\Delta\sigma_{gb}$ is presented in Table 4.

Compared with that of the as-rolled Al-10wt% Mg alloy, after annealing at 75 °C, the dislocation density and Mg solute content slightly decrease from 1.85×10^{14} m^{-2} to 1.44×10^{14} m^{-2} and from 9.68wt% to 9.52wt% , respectively; $\bar{d}_R$ increases from 176.2 nm to 224.1 nm, leading to slight decrease in $\Delta\sigma_d$ from 94.4 MPa to 83.5 MPa, in $\Delta\sigma_{ss}$ from 183.5 MPa to 180.1 MPa, and in $\Delta\sigma_{gb}$ from 142.9 MPa to 126.8 MPa; YS also decreases by ~7%. After annealing at 100 °C, the dislocation density decreases to 1.23×10^{14} m^{-2}, Mg solute content decreases to 9.02wt%, and $\bar{d}_R$ increases to 256.3 nm, leading to the decreased $\Delta\sigma_d$ of 77.1 MPa, $\Delta\sigma_{ss}$ of 169.3 MPa, and $\Delta\sigma_{gb}$ of 118.5 MPa; YS also decreases by ~13%. After annealing at 150 °C, the dislocation density further decreases to 7.04×10^{13} m^{-2}, Mg solute content decreases to 8.88wt%, and $\bar{d}_R$ increases to 388.1 nm, leading to the decreased $\Delta\sigma_d$ of 58.3 MPa, $\Delta\sigma_{ss}$ of 166.3 MPa, and $\Delta\sigma_{gb}$ of 96.3 MPa; thus YS decreases greatly by ~24%. The deviation between the calculated and experiment values of decreased percentages in YS is large, which is primarily attributable to the uncertainty of the material constants in the above equations for calculation of the contributions of the three strengthening mechanisms, including H and n for $\Delta\sigma_{ss}$, M and α_1 for $\Delta\sigma_d$, and K for $\Delta\sigma_{gb}$. Despite the deviation, both the calculated and experiment results show similar variation tendencies of YS of alloys after

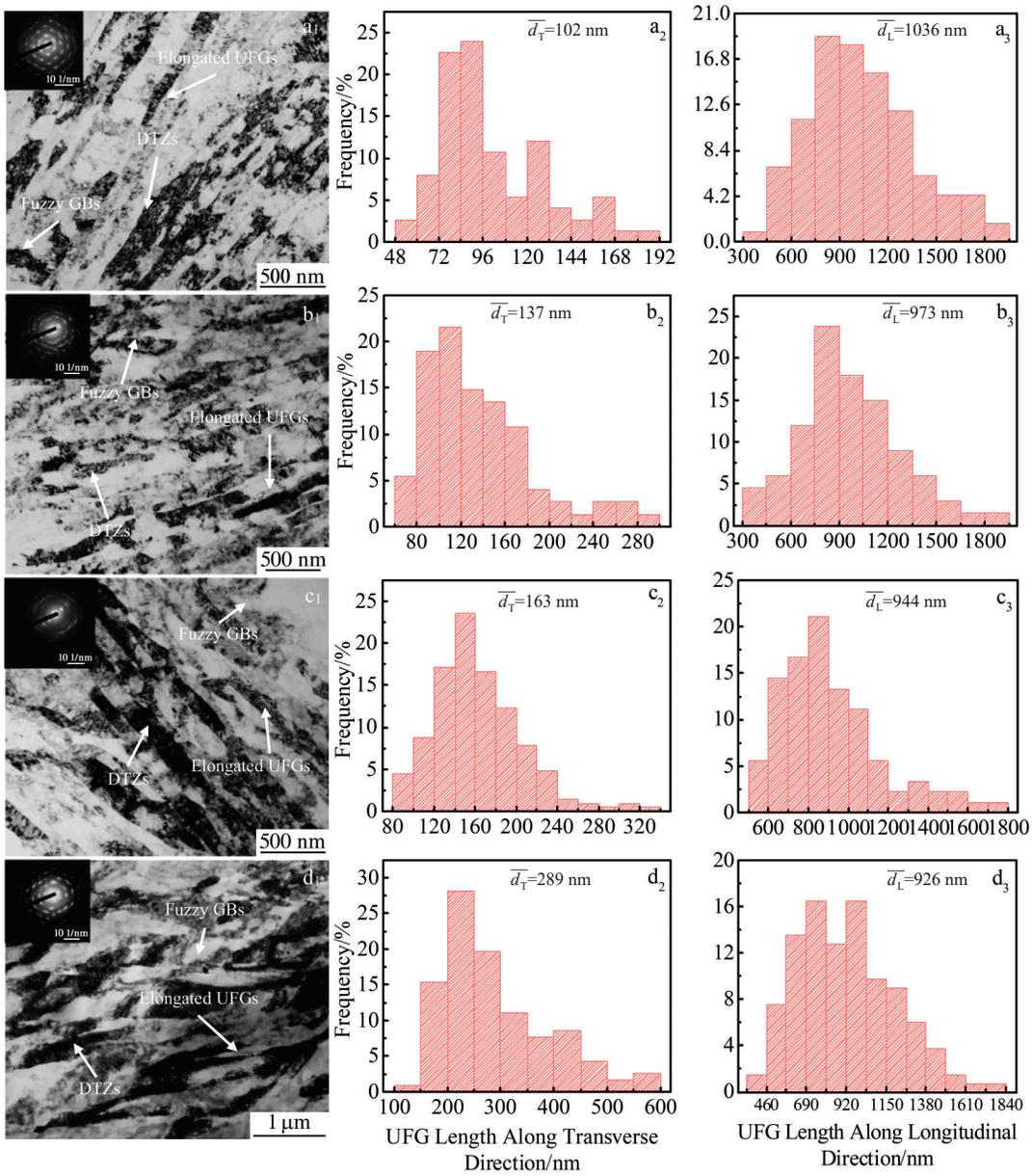

Fig.4 TEM microstructures (a_1~d_1) and length distribution of elongated UFGs along transverse (a_2~d_2) and longitudinal (a_3~d_3) directions in as-rolled (a_1~a_3), 75 °C/annealed (b_1~b_3), 100 °C/annealed (c_1~c_3), and 150 °C/annealed (d_1~d_3) Al-10wt% Mg alloys

Table 4 Contributions of different strengthening mechanisms in as-rolled and annealed Al-10wt% Mg alloys

Treatment	$\Delta\sigma_d$/MPa	$\Delta\sigma_{ss}$/MPa	$\Delta\sigma_{gb}$/MPa	$\overline{d}_R$/nm
As-rolled	94.4	183.5	142.9	176.2
75 °C/annealed for 1 h	83.5	180.1	126.8	224.1
100 °C/annealed for 1 h	77.1	169.3	118.5	256.3
150 °C/annealed for 1 h	58.3	166.3	96.3	388.1

annealing at 75~150 °C.

Two factors critically affect the dislocation accumulation and thus the work hardening and ductility during tensile tests in the as-rolled and annealed Al-10wt% Mg alloys: the preexisting dislocation density before tensile tests[36] and Mg solute content[7,36]. With the lower preexisting dislocation density before tensile tests, the tendency of dynamic recovery during test is reduced, which is beneficial to the dislocation accumulation, thus improving the work-hardening effect. With the lower Mg solute content, the impedance of Mg solute against dynamic recovery during test is reduced, facilitating the dislocation annihilation and decreasing the work-hardening effect. Due to the slight decrease in Mg solute content during annealing at 75~150 ° C, the increased dislocation accumulation caused by the decreased preexisting dislocation density overwhelms the increased dislocation annihilation induced by the reduced Mg solute content. Thus, compared with the as-rolled Al-10wt% Mg alloy, after annealing at 75 ° C, the slight decrease in preexisting dislocation density leads to slight increase in elongation by

~16%. After annealing at 100 and 150 °C, the preexisting dislocation density is decreased more, so the alloys can yield higher elongation incresed by ~72% and ~83%, respectively.

3 Conclusions

1) The microstructures of Al-10wt% Mg alloys after rolling and annealing at 75~150 °C consist of elongated ultra-fine grains (UFGs) with a high density of dislocations and a very low amount of Al_3Mg_2 phase without dispersion. With increasing the annealing temperature, the width of elongated UFGs is increased, the length of elongated UFGs is slightly decreased, and the dislocation density is also decreased.

2) Compared with those of the as-rolled Al-10wt% Mg alloy, after annealing at 75 °C, the dislocation density and Mg solute concentration slightly decrease, the average boundary spacing of elongated grains slightly increases, and thus the dislocation, solid-solution, and grain boundary (GB) strengthening slightly decrease, leading to a slight decrease in yield strength (YS) by ~8% and ultimate tensile strength (UTS) by ~1%. After annealing at 100 °C, the dislocation density and Mg solute content further decrease, the average boundary spacing of elongated grains further increases, and therefore the dislocation, solid-solution, and GB strengthening further decrease, resulting in further decrease in YS by ~23% and UTS by ~12%. After annealing at 150 °C, the dislocation density and Mg solute content shows a larger reduction, the average boundary spacing of elongated grains shows a greater increment, and hence the dislocation, solid-solution, and GB strengthening decrease more sharply, leading to an obvious decline in YS by ~33% and UTS by ~12%. After annealing at 200 °C, YS and UTS decrease by ~35% and ~10%, respectively, compared with those of as-rolled alloys.

3) The preexisting dislocation density before tensile tests dominates the dislocation storage ability during tensile tests and thus the work-hardening and ductility, due to slight change in Mg solute content during annealing. After annealing at 75 °C, a slight decrease in dislocation density leads to a slight increase in elongation by ~16%, compared with that of as-rolled alloys. After annealing at 100 °C, the further decreased dislocation density yields the further increase in elongation by ~72%. After annealing at 150 °C, the further decrease in dislocation density results in much more increase in elongation by ~83%. After annealing at 200 °C, the elongation decreases, compared with that of alloys after annealing at 150 °C, due to the Al_3Mg_2 precipitation.

4) With YS of 331 MPa and elongation of 11.9%, the good combination of strength and ductility is achieved for Al-10wt% Mg alloys by annealing at 100 °C. In contrast, the required mechanical properties cannot be attained by annealing at temperatures lower than 75 °C or higher than 150 °C.

References

1 Chen Kehua, Liang Wei, Wang Shunqi *et al*. *Rare Metal Materials and Engineering*[J], 2010, 39(2): 352

2 Engler O. *Materials Science and Engineering A*[J], 2014, 618: 654

3 Lee S, Yeh J. *Materials Science and Engineering A*[J], 2007, 460-461: 409

4 Mostafaei M A. *Journal of Alloys and Compounds*[J], 2019, 811: 151 997

5 Ninomiya M, Ohte R, Uesugi T *et al*. *Materials Letters*[J], 2019, 245: 218

6 Zha M, Li Y J, Mathiesen R H *et al*. *Materials Science and Engineering A*[J], 2013, 586: 374

7 Zha M, Li Y J, Mathiesen R H *et al*. *Acta Materialia*[J], 2015, 84: 42

8 Huskins E L, Cao B, Ramesh K T. *Materials Science and Engineering A*[J], 2010, 527(6): 1292

9 Miller W S, Zhuang L, Bottema J *et al*. *Materials Science and Engineering A*[J], 2000, 280(1): 37

10 Chen Y J, Chai Y C, Roven H J *et al*. *Materials Science and Engineering A*[J], 2012, 545: 139

11 Zha M, Meng X T, Zhang H M *et al*. *Journal of Alloys and Compounds*[J], 2017, 728: 872

12 Jang D H, Park Y B, Kim W J. *Materials Science and Engineering A*[J], 2019, 744: 36

13 Courtney T H. *Mechanical Behavior of Materials*[M]. Waveland: Long Grove, 2000

14 Ni S, Wang Y B, Liao X Z *et al*. *Scripta Materialia*[J], 2011, 64(4): 327

15 Ma E, Wang Y M. *Applied Physics Letters*[J]. 2004, 85(21): 4932

16 Lee B H, Kim S H, Park J H *et al*. *Materials Science and Engineering A*[J], 2016, 657: 115

17 Feng L, Li Z W, Huang C. *Metals*[J], 2019, 9(7): 759

18 Liu Z B, Sun J N, Yan Z G *et al*. *Materials Science and Engineering A*[J], 2021, 806: 140 806

19 Wen X C, Guo L, Bao Q P *et al*. *Journal of Alloys and Compounds*[J], 2020, 832: 154 995

20 Valiev R Z, Enikeev N A, Murashkin M Y *et al*. *Scripta Materialia*[J], 2010, 63(9): 949

21 Alexander H P, Klug L. *X-ray Diffraction Procedures for Polycrystalline and Amorphous Materials*[M]. New York: John Wiley and Sons, 1974

22 Williamson G K, Smallman R E. *Philosophical Magazine*[J], 1956, 1(1): 34

23 Smallman R E, Westmacott K H. *Philosophical Magazine*[J], 1957, 2(17): 669

24 Davis J R. *Aluminium and Aluminum Alloys*[M]. Cleveland: ASM International, 1993

25 Lumley R. *Fundamentals of Aluminium Metallurgy: Production, Processing and Applications*[M]. Cambridge: Woodhead Publishing, 2011

26 Dierke H, Krawehl F, Graff S *et al*. *Computational Materials Science*[J], 2007, 39(1): 106

27 Kovács Z, Lendvai J, Vörös G. *Materials Science and*

Engineering A[J], 2000, 279(1): 179
28 Prangnell P B, Hayes J S, Bowen J R *et al*. *Acta Materialia*[J], 2004, 52(11): 3193
29 Jazaeri H, Humphreys F J. *Acta Materialia*[J], 2004, 52(11): 3251
30 Ryen Ø, Holmedal B, Nijs O *et al*. *Metallurgical and Materials Transactions A*[J], 2006, 37(6): 1999
31 Ma K K, Hu T, Yang H *et al*. *Acta Materialia*[J], 2016, 103: 153
32 Stoller R E, Zinkle S J. *Journal of Nuclear Materials*[J], 2000, 283-287(1): 349
33 Ashby M F. *Philosophical Magazine*[J], 1970, 21(170): 399
34 Cheng S, Spencer J A, Milligan W W. *Acta Materialia*[J], 2003, 51(13): 4505
35 Hughes D A, Hansen N. *Acta Materialia*[J], 2000, 48(11): 2985
36 Ni S, Wang Y B, Liao X Z *et al*. *Scripta Materialia*[J], 2011, 64(4): 327

低温退火加工硬化 Al-10% Mg 合金的显微组织特点和力学行为

散展翼[1]，刘生发[1]，刘志波[1]，林耀军[1]，刘满平[2]
(1. 武汉理工大学 材料科学与工程学院，湖北 武汉 430070)
(2. 江苏大学 材料科学与工程学院，江苏 镇江 212013)

摘 要：研究了冷轧减薄率为75%的Al-10% Mg（质量分数）合金在75~150 ℃下退火的显微组织特点和力学行为。轧制态和退火态Al-10% Mg合金的特征是晶粒细长，位错密度高，Al_3Mg_2相含量极低，且无弥散分布的Al_3Mg_2相。随着退火温度的升高，细长晶粒的宽度增加，位错密度减小。在75~150 ℃退火后，相比于轧制态合金，其屈服强度降低8%~33%，极限抗拉伸强度降低1%~12%，延伸率增加16%~83%。此外，分析了各种强化机制对屈服强度的贡献，以及原有位错和Mg溶质对塑性的贡献。

关键词：铝镁合金；冷轧；退火；强度；韧性

作者简介：散展翼，男，1995年生，硕士，武汉理工大学材料科学与工程学院，湖北 武汉 430070，E-mail：1297539664@qq.com